2006

Wavelet Analysis in Virtual Colonoscopy

Sharon Greenblum
National Institutes of Health

Jiang Li
National Institutes of Health, jli@odu.edu

Adam Huang
National Institutes of Health

Ronald M. Summers
National Institutes of Health

Armando Manduca (Ed.)

See next page for additional authors

Original Publication Citation

Greenblum, S., Li, J., Huang, A., & Summers, R. M. (2006) Wavelet analysis in virtual colonoscopy. In A. Manduca & A.A. Amini (Eds.), *Medical Imaging 2006: Physiology, Function, and Structure from Medical Images, Proceedings of SPIE Volume 6143* (614336). SPIE. https://doi.org/10.1117/12.655680

Wavelet Analysis in Virtual Colonoscopy

Sharon Greenblum, Jiang Li, Adam Huang and Ronald M. Summers[1]

Diagnostic Radiology Department, Warren Grant Magnuson Clinical Center,
National Institutes of Health

ABSTRACT

The computed tomographic colonography (CTC) computer aided detection (CAD) program is a new method in development to detect colon polyps in virtual colonoscopy. While high sensitivity is consistently achieved, additional features are desired to increase specificity. In this paper, a wavelet analysis was applied to CTCCAD outputs in an attempt to filter out false positive detections.

52 CTCCAD detection images were obtained using a screen capture application. 26 of these images were real polyps, confirmed by optical colonoscopy and 26 were false positive detections. A discrete wavelet transform of each image was computed with the MATLAB wavelet toolbox using the Haar wavelet at levels 1-5 in the horizontal, vertical and diagonal directions. From the resulting wavelet coefficients at levels 1-3 for all directions, a 72 feature vector was obtained for each image, consisting of descriptive statistics such as mean, variance, skew, and kurtosis at each level and orientation, as well as error statistics based on a linear predictor of neighboring wavelet coefficients. The vectors for each of the 52 images were then run through a support vector machine (SVM) classifier using ten-fold cross-validation training to determine its efficiency in distinguishing polyps from false positives.

The SVM results showed 100% sensitivity and 51% specificity in correctly identifying the status of detections. If this technique were added to the filtering process of the CTCCAD polyp detection scheme, the number of false positive results could be reduced significantly.

Keywords: virtual colonoscopy, wavelet, classifiers, computer aided detection

1. INTRODUCTION

Colon cancer is one of the most common, yet most treatable forms of cancer. Early detection and removal of colon polyps (small round growths in the colon lining) is best way to approach treatment; therefore, a quick, simple, non-intrusive detection method is very important [1]. Current colonoscopy methods involving anesthesia and a video colonoscopy are not optimal; however a promising new technique is virtual colonoscopy. With this technique, polyps are identified from CT scans using a computer-aided detection system. The computed tomographic colonography (CTC) computer aided detection (CAD) program being developed identifies polyps based on curvature, and while it achieves high sensitivity, more work is needed to increase specificity by filtering out false positives [2].

Wavelets are a relatively new area of research with widespread applications to the scientific world [3]. Wavelets use a multi-scale, multi-orientation approach to describing signals and images by separating them into layers of detail and low-resolution approximations. A discrete wavelet analysis of an image will output wavelet coefficients in the horizontal, vertical, and diagonal directions at specified levels of analysis. Statistics gathered from these coefficients can provide a powerful tool in image comparison.

A wavelet-like analysis was recently used to identify forgeries in valuable paintings by comparing the artists' signature pattern of brushstrokes [4]. In this paper, we apply a similar technique to virtual colonoscopy images in order to distinguish real polyps from false positives.

[1]Further author information: (Send correspondence to Ronald M. Summers)
Address: Building 10 Room 1C660, 10 Center Drive MSC 1182, Bethesda, MD 20892-1182
E-mail: rms@nih.gov Website: http://www.cc.nih.gov/drd/summers.html

Medical Imaging 2006: Physiology, Function, and Structure from Medical Images,
edited by Armando Manduca, Amir A. Amini, Proc. of SPIE Vol. 6143,
614336, (2006) · 1605-7422/06/$15 · doi: 10.1117/12.655680

2. METHODS

26 virtual colonoscopy cases were obtained, each containing at least one known polyp, whose position was previously determined by optical colonoscopy. The cases were picked at random from a database consisting of the supine scans of patients with 6-9 mm polyps not under fluid. Each case was run through an existing CTCCAD program (Fig.1). The program scans the colon and returns a list of detections with corresponding images. A screen capture tool was used to save a bitmap image of the en face endoluminal view of each detection. The images were 192 x 222 pixels, plus or minus one pixel. For each case, one true polyp (Fig. 2a) and one false positive detection (Fig. 2b) were used. The 52 bitmap images were then converted to grayscale and analyzed using MATLAB version 6.5's wavelet toolbox. A 2D discrete wavelet decomposition was performed using the Haar wavelet basis at levels 1-5 in the horizontal, vertical, and diagonal directions which resulted in 16 subband coefficients for each image. Fig.3 shows one example of the wavelet transformation performed at levels 1-3.

The wavelet decomposition of an image yielded a set of wavelet coefficients which describe both the large and small-scale shape features of the surface. Following the method of Lyu et al. [4], four descriptive statistics were computed at 1-3 levels for each orientation from these coefficients: mean, variance, skew, and kurtosis.

Then, a linear predictor function was used to compute the second order error statistics for each coefficient subband at levels 1-3, based on the linear prediction error of each coefficient, in the subband by its spatial, orientation, and scale neighbors. First, the 7 numerically closest coefficient neighbors were found iteratively from among its 80 neighbors. For example, at a vertical orientation at scale i, the neighbors of coefficient $V_i(x,y)$ were defined as:

$$\begin{aligned} &V_i(x-c_x, y-c_y), H_i(x-c_x, y-c_y), D_i(x-c_x, y-c_y), \\ &V_{i+1}(\frac{x}{2}-c_x, \frac{y}{2}-c_y), H_{i+1}(\frac{x}{2}-c_x, \frac{y}{2}-c_y), D_{i+1}(\frac{x}{2}-c_x, \frac{y}{2}-c_y), \\ &V_{i+2}(\frac{x}{4}-c_x, \frac{y}{4}-c_y), H_{i+2}(\frac{x}{4}-c_x, \frac{y}{4}-c_y), D_{i+2}(\frac{x}{4}-c_x, \frac{y}{4}-c_y), \end{aligned} \tag{1}$$

where $c_x = \{-1,0,1\}$ and $c_y = \{-1,0,1\}$, and $V_i(x,y)$ was excluded. Here V_i, H_i and D_i denote the wavelet coefficients in the vertical, horizontal and diagonal directions at level i. The seven closest neighbors were determined by finding the minimum difference between these neighbors and the original coefficient, and repeating the process 6 times.

Then, a column vector $\vec{V}$ was created containing the values of all original coefficients in the subband. A matrix Q was also created, composed of 7 columns of closest neighbor coefficients for the corresponding coefficient in the subband. Using the linear predictor $\vec{V} = Q\vec{w}$, a column of predictor coefficients $\vec{w}$ was computed by

$$\vec{w} = (Q^T Q)^{-1} Q^T \vec{V} \tag{2}$$

The errors in the linear predictor were the residuals

$$\vec{E} = (\vec{V} - Q\vec{w})^2 \tag{3}$$

The same four statistics (mean, variance, skew, kurtosis) were computed for the subband and this process was repeated for each subband at levels 1-3. The feature extraction method in this paper gives a 72 feature vector for each image.

Next, feature selection and training of a committee classifier were performed. Feature selection was done using a genetic algorithm [5]. Ten-fold cross-validation training was done using a support vector machine (SVM) classifier, ultimately generating a 7 member SVM committee classifier using 4 features each.

This procedure was carried out on 3 sets of data, varying only in color scheme and lighting attributes, in order to determine which images were most compatible with a wavelet analysis. One data set contained black and white images (Fig. 4a), another contained true color images with specular lighting added (Fig.4c), and the third contained true color images with all except diffuse lighting removed (Fig. 4e).

The classifier produced a specificity reading for each data set, representing the percent of false positives that were correctly identified when the classifier was run at a sensitivity level allowing correct identification of all polyps. An average ROC curve from 10 bootstraps was also created to visualize these results, with mean area under the ROC curve (AUC) representative of the efficiency of the classifier for the particular data set.

3. RESULTS

The following table shows the classifier results for the three data sets. The classifier performed the best with the diffuse lighting data, correctly identifying about ½ of the false positive detections at a sensitivity of 100%. Mean ROC curves for each data set are shown in figs. 4b, 4d, and 4f, and the mean area under the curve (AUC) as well as the standard deviation in this measurement are included in the table below. The results again support the conclusion that the diffuse lighting pictures are best suited to this type of analysis.

Table 1

Data set	Sensitivity	Specificity	AUC	Stand. Dev.
Black and white	100% (27/27)	26.8% (8/27)	0.81	0.067
Specular	100% (26/26)	34.5% (10/26)	0.92	0.046
Diffuse	100% (26/26)	51.4% (13/26)	0.93	0.047

Upon reviewing the misclassified images, we found that many of the incorrectly identified false positives contained shapes similar to polyps, or contained no identifiable shapes at all. One case, present in the black and white data set, was left out of the specular and diffuse data sets due to an error in image processing.

4. CONCLUSION

Ultimately the idea behind a wavelet analysis is to capture some of the information so readily apparent to the human eye, such as shape and contour, in a form that can be understood and manipulated by a computer. Since the wavelet analysis is dependent on the visual properties of an image, the detection images must be modified to include full color and only diffuse lighting in order to produce the best classification. This seems reasonable since it is in these images, with minimal extraneous shadows and reflections and maximum range of shading, that the human eye is best able to discern a polyp structure. The wavelet decomposition of virtual colonoscopy images is able to distinguish real polyps from many non-polyp CTCCAD detections, enabling exclusion of about ½ of the non-polyp detections. This technique, if added to the filtering process of the CTCCAD program, could aid the radiologist in expediting the CT reading process and could be useful in preventing unnecessary optical colonoscopies.

ACKNOWLEDGEMENTS

We thank Dr. Andrew Dwyer, MD for reviewing this manuscript, and Perry Pickhardt, Richard Choi and William Schindler for supplying CT colonography data. This research was supported by the Intramural Research Program of the NIH, Warren G. Magnuson Clinical Center.

REFERENCES

1. D. M. Eddy, “Screening for colorectal cancer,” *Ann. Intern. Med.*, vol.113, pp. 373–384, 1990.

2. R. M. Summers, C. F. Beaulieu, L. M. Pusanik, J. D. Malley, R. B. Jeffrey, D. I. Glazer, and S. Napel, “Automated polyp detector for CT colonography: Feasibility study,” *Radiology*, vol. 216, no. 1, pp. 284–290, 2000.

3. B. B. Hubbard, *The world according to wavelets : the story of a mathematical technique in the making*, 2nd ed. Wellesley, Mass: A.K. Peters, 1998.

4. S. Lyu, D. Rockmore, and H. Farid, "A digital technique for art authentication, "*Proc Natl Acad Sci U S A*, vol. 101, pp. 17006-10, 2004.

5. M. Miller, A. K. Jerebko, J. D. Malley, and R. M. Summers RM, "Comparison of stochastic vs. heuristic feature subset selection methods for improving classification algorithms in computer-aided detection," *Proceedings of SPIE*, vol. 5031, pp. 102-110, 2003.

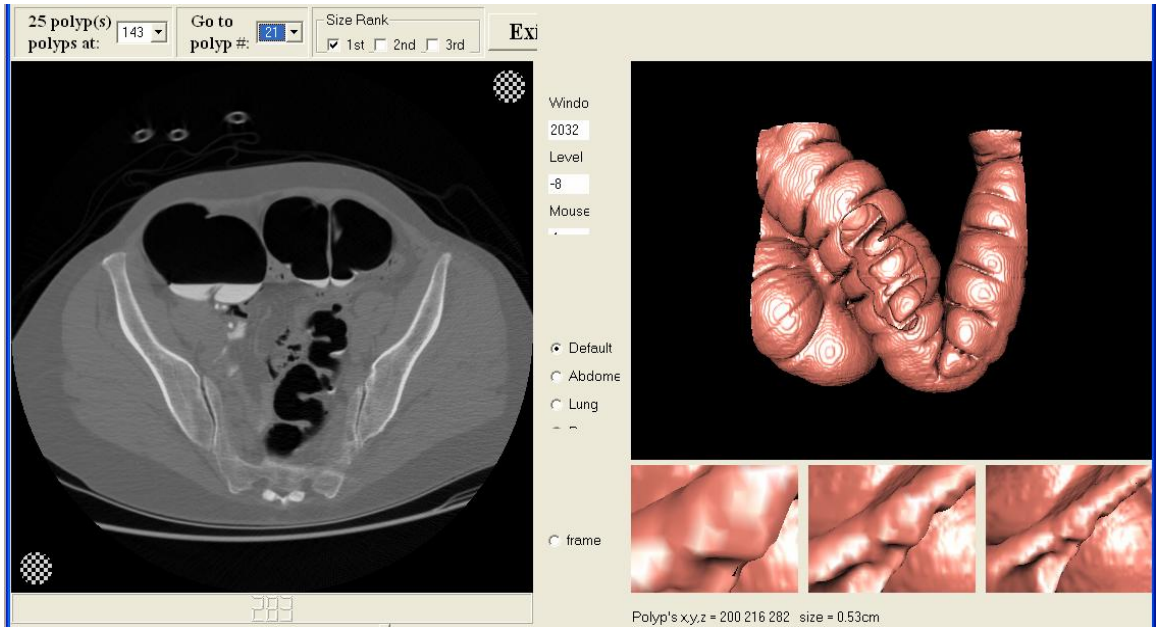

Figure 1. CTCCAD display window

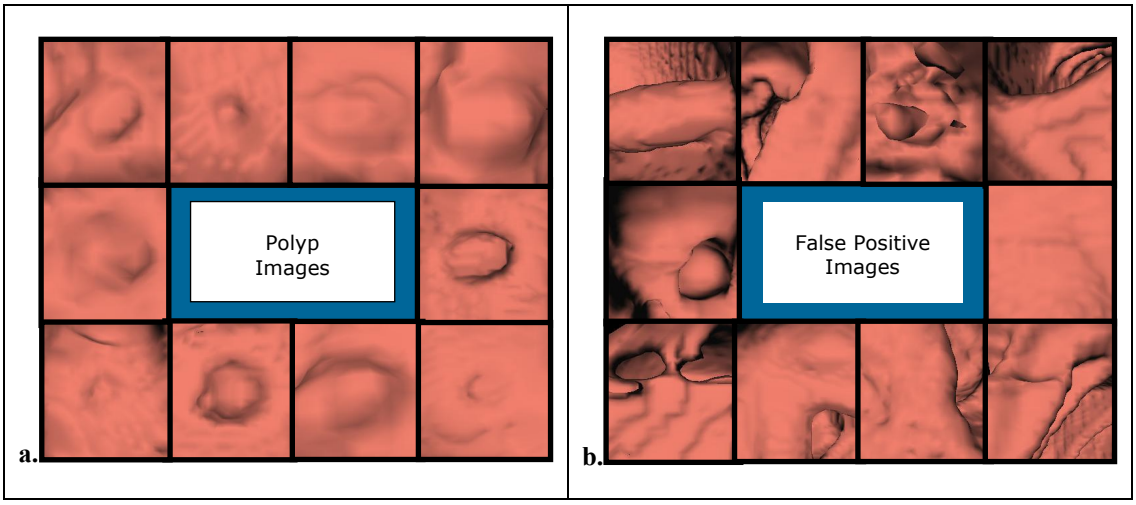

Figure 2. CTCCAD detection examples

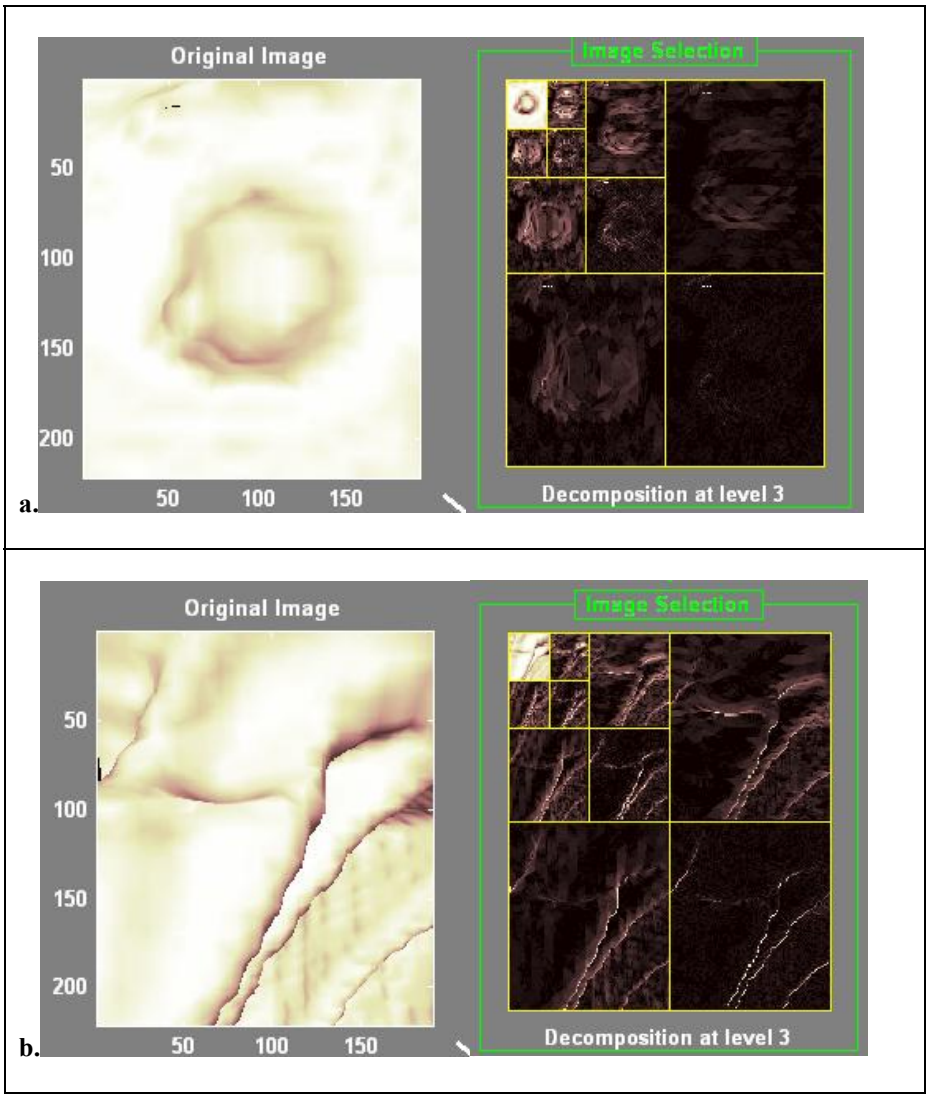

Figure 3. MATLAB visualization of wavelet decompositions for *a.* a polyp, and *b.* a false positive detection

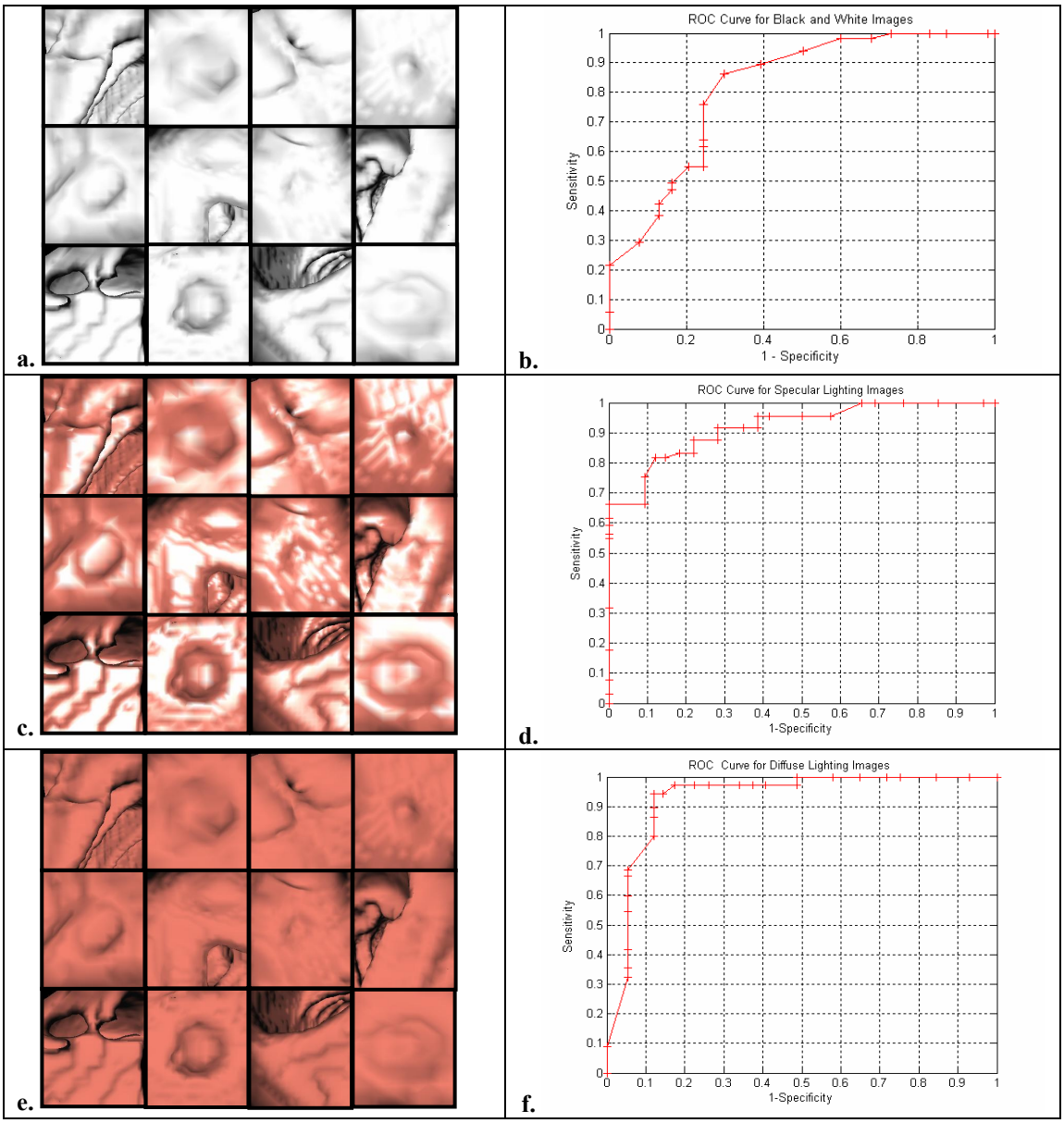

Figure 4. Mosaic of alternating polyp and false positive images under different color and lighting conditions and associated ROC curves. *a, b*: black and white; *c, d*: with added specular lighting; *e, f*: with diffuse lighting only.

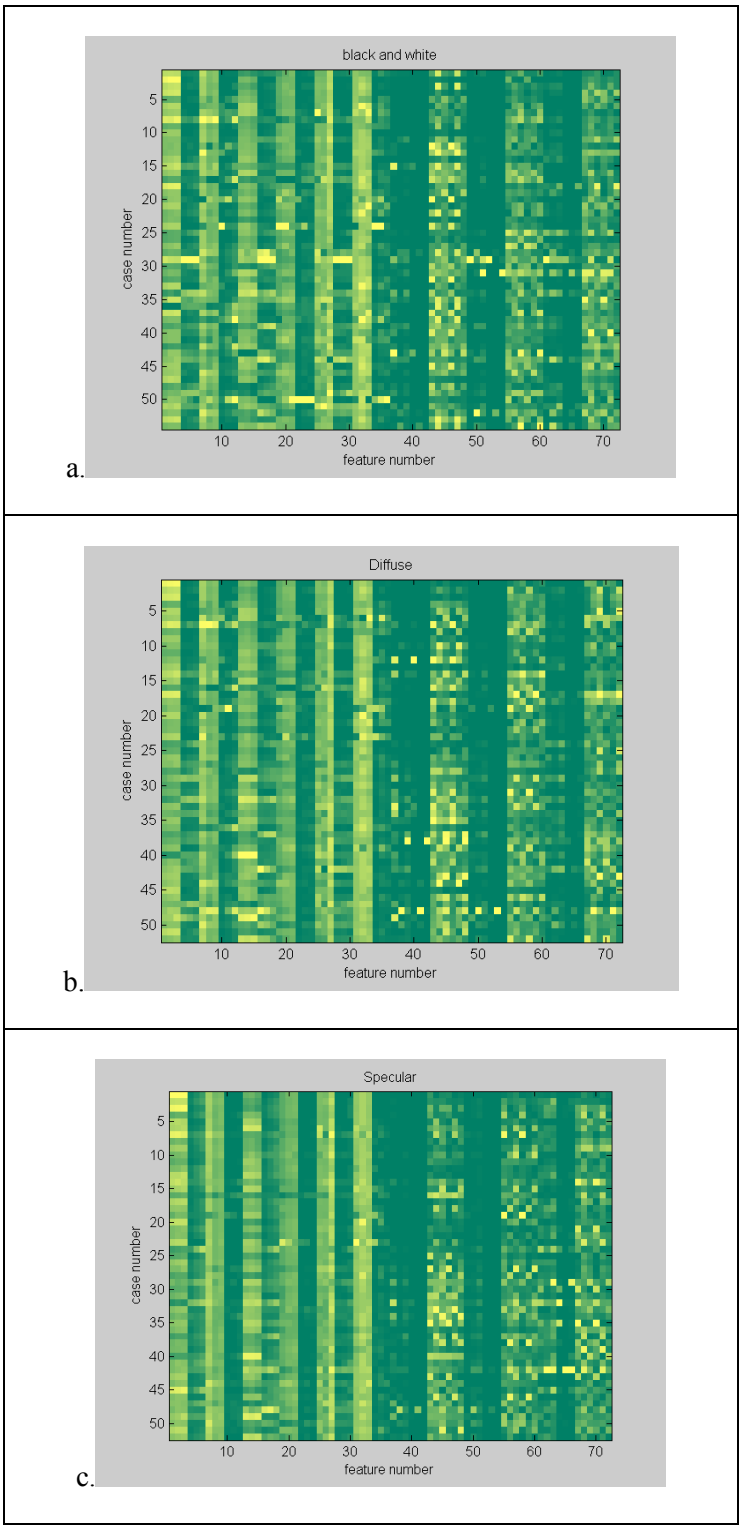

Figure 5. Graphic illustration of wavelet statistics for *a*. black and white, *b*. specular, and *c*. diffuse data. Green represents the lowest value for that statistic, and yellow the highest. The top portion of the graphs are the true positives (case numbers 1-26), while the bottom portion of the graphs are the false positives (case numbers 27-52).